

## Slow Proton and $\Delta^{++}$ Production in $K^+p$ Interactions at 70 GeV/c

M. Barth<sup>1</sup>, C. De Clercq<sup>2</sup>, E. De Wolf<sup>3</sup>, J. J. Dumont<sup>1</sup>, D. P. Johnson<sup>2</sup>, J. Lemonne, P. Peeters  
Inter-University Institute for High Energies, B-1050 Brussels, Belgium

R. Contri, H. Drevermann, L. Gerdyukov<sup>4</sup>, Y. Goldschmidt-Clermont, G. Harigel, J. Joensuu<sup>5</sup>, C. Milstene<sup>6</sup>, J. P. Porte, R. T. Ross, M. Spyropoulou-Stassinaki<sup>7</sup>  
CERN, CH-1211 Geneva 23, Switzerland

C. Caso, F. Fontanelli, R. Monge, S. Squarcia, U. Trevisan  
Sezione INFN and Istituto di Scienze Fisiche, I-16132 Genova, Italy

J. F. Baland, J. Beaufays, F. Grard, J. Hanton  
Faculté des Sciences, Université de l'Etat, B-7000 Mons, Belgium

P. A. Van der Poel, L. Gatignon, W. Kittel, W. J. Metzger, D. J. Schotanus, A. Stergiou, R. T. Van de Walle  
University of Nijmegen, Nijmegen, The Netherlands<sup>8</sup>

Y. Belokopitov, V. Brizgalov, P. Chliapnikov, A. Fenuyk, V. Kubic, E. Krytchenko, S. Lugovsky, V. Nikolaenko, J. Petrovikh, V. Ronjin, O. Tchikilev, V. Yarba, V. Zjigunov  
Institute for High Energy Physics, Serpukhov, USSR<sup>9</sup>

Received 21 September 1980

**Abstract.** The inclusive inelastic processes  $K^+p \rightarrow pX^+$  and  $K^+p \rightarrow \Delta^{++}X^0$  are studied at an incident momentum of 70 GeV/c. The data comes from the Big European Bubble Chamber BEBC filled with hydrogen, exposed to an rf separated  $K^+$  beam at the CERN SPS accelerator. The inclusive cross section for protons with laboratory momentum  $p_{\text{LAB}} \leq 1.2$  GeV/c is equal to  $(6.1 \pm 0.1)$  mb. Inclusive  $\Delta^{++}$ -production is studied for  $|t_{p,\Delta}| < 1.0$  (GeV/c)<sup>2</sup>. Comparisons are made with other  $K^+p$  data and with  $pp$  data at 69 GeV/c. Evidence is found for Pomeron exchange at the beam vertex both for slow proton and  $\Delta^{++}$ -production as

well as for absorptive pion exchange at the  $(p, \Delta^{++})$  vertex.

### 1. Event Selection

This paper presents results on the inclusive inelastic reactions:

$$\begin{aligned}
 K^+p \rightarrow p + X^+ & \text{ with } p_{\text{LAB}}(p) < 1.2 \text{ GeV/c}, & (1) \\
 K^+p \rightarrow (p\pi^+) + X^0 & \text{ with } |t_{p,\pi^+}| < 0.6 \text{ (GeV/c)}^2 \\
 & \text{and } 1.16 < M_{p\pi^+} < 1.32 \text{ GeV/c}^2, & (2)
 \end{aligned}$$

and

$$K^+p \rightarrow \Delta^{++} + X^0 \text{ with } |t_{p,\Delta}| < 0.6 \text{ (GeV/c)}^2 \quad (3)$$

studied at a laboratory momentum of 70 GeV/c. The sample used for this analysis ( $\sim 27,000$  events) corresponds to a sensitivity of  $\sim 1.7$  events/ $\mu\text{b}$  and is obtained from an exposure at the CERN SPS accelerator of the bubble chamber BEBC, filled with hydrogen, to an rf-separated beam of  $K^+$  mesons. The  $\pi^+$  and  $\mu^+$  contaminations of the beam were determined to be small,  $\sim 2\%$  and  $\sim 1\%$ , respectively. Details

<sup>1</sup> Chercheur IISN, Belgium

<sup>2</sup> Navorser IIKW, Belgium

<sup>3</sup> Bevoegdverklaard Navorser NFWO; also at Universitaire Instelling Antwerpen

<sup>4</sup> On leave from the I.H.E.P., Serpukhov, USSR

<sup>5</sup> Visitor from the University of Helsinki

<sup>6</sup> Visitor from the University of Tel-Aviv

<sup>7</sup> Visitor from the University of Athens

<sup>8</sup> Supported in part by the joint research program of FOM and ZWO

<sup>9</sup> Participating under the term of the 1967 Agreement between CERN and the USSR State Committee for the Utilization of Atomic Energy and the Protocols

**Table 1.** Total and topological inclusive cross sections (in mb) for the reaction  $K^+p \rightarrow pX^+$  and  $K^+p \rightarrow \Delta^{++}X^0$  at 70 GeV/c

Charged topology	Total	2	4	6	8	10	12	$\geq 14$
$K^+p \rightarrow pX^+$ $p_{\text{LAB}}(p) < 1.2 \text{ GeV}/c$	$6.1 \pm 0.1$	$0.94 \pm 0.03$	$2.29 \pm 0.07$	$1.6 \pm 0.03$	$0.85 \pm 0.03$	$0.32 \pm 0.02$	$0.076 \pm 0.008$	$0.04 \pm 0.02$
$K^+p \rightarrow (p\pi^+)X^0$ $ t_{p,(p\pi^+)}  < 0.6 \text{ (GeV}/c)^2$ $(1.16 < M(p\pi^+) < 1.32) \text{ GeV}/c^2$	$0.82 \pm 0.02$	$0.041 \pm 0.005$	$0.299 \pm 0.015$	$0.268 \pm 0.013$	$0.156 \pm 0.010$	$0.043 \pm 0.006$	$0.008 \pm 0.002$	$0.001 \pm 0.001$

concerning the exposure conditions can be found in [1]. Approximately 60,000 frames were doubly scanned for all topologies and the events recorded were subsequently measured and passed through the HYDRA geometry program. The scanning efficiency was  $\sim 85\%$  for 2-prong interactions and close to 100% for all other topologies. For part of the primary event sample ( $\sim 80\%$ ), the bubble density of all positive tracks with momentum less than 1.2 GeV/c and with mass-dependent fits compatible both with the  $\pi^+$  and the proton hypothesis, was checked on the scanning table. A reliable identification of protons by this visual method appeared to be possible up to a momentum of 1.2 GeV/c. This fully checked sample was used to calibrate the efficiency of an automatic proton identification method, based on the mass-dependent geometry information, which was applied to the remaining events. The efficiency of this automatic identification method is higher than 90% for proton momenta below 900 MeV/c and decreases to 30% at 1.2 GeV/c.

Elastic events were discarded from the sample by cuts on the missing mass squared  $M_X^2$  to the proton and on the difference  $\Delta\theta$  between the measured laboratory angle of the fast particle and its value calculated from the measured momentum of the identified proton assuming an elastic collision. The cuts  $|\Delta\theta| < 6 \text{ mrad}$  and  $M_X^2 < 1.0 \text{ (GeV}/c^2)^2$  were used. A total of 26,893 well measured inelastic events was selected. In 8835 of those, a slow proton was identified either visually or automatically.

## 2. Total and Topological Inclusive Cross Sections

In order to estimate the inclusive cross sections for reactions (1)–(3) we have renormalized the charged particle multiplicity distribution of the primary interactions retained for this analysis, to the topological cross sections determined in a previous study of our data [1]. By this procedure we implicitly account for scanning and throughput efficiencies which are independent of the presence of a slow proton. The effect of the loss of very short proton tracks was estimated from an exponential extrapolation of the four momentum transfer  $t' = |t - t_{\text{min}}|$  distributions for different topo-

logies and amounts to less than 2% of all inelastic events. The total and topological cross sections for reaction (1) are given in Table 1. The total cross section is found to be  $6.1 \pm 0.1 \text{ mb}$ , i.e. almost equal to the values found in  $K^+p$  interactions at 16 GeV/c [2] and 32 GeV/c [3]. It represents  $\sim 38\%$  of the  $K^+p$  inelastic cross section. The energy dependence of the topological cross sections for this reaction is illustrated in Fig. 1. The 2-prong and 4-prong cross sections decrease in the incident momentum range from 16 to 70 GeV/c while the cross sections of higher charged multiplicities still increase with increasing energy. We can conclude that, as observed at lower energies, there is still a tendency for the events of reaction (1) to be mainly restricted to the lower charged multiplicities but a clear shift towards higher topologies is already evident.

The inclusive  $(p\pi^+)$  invariant mass  $M_{p\pi^+}$  distribution for events with an identified proton and  $|t_{p,(p\pi^+)}| < 0.6 \text{ (GeV}/c)^2$  is shown in Fig. 2. Each charged positive particle, except the one identified as a proton, was in turn called a  $\pi^+$ . The background level is seen to be relatively small in the  $\Delta^{++}$ -resonance region defined as  $1.16 < M_{p\pi^+} < 1.32 \text{ GeV}/c^2$  \*. The total and topological cross sections for reaction (2) are given in Table 1. The value of the cross section for this reaction found in this experiment,  $(0.82 \pm 0.02) \text{ mb}$  is of the same order of magnitude as that found at 32 GeV/c [4].

The inclusive  $\Delta^{++}$ -cross section for  $|t_{p,\Delta}| < 0.6 \text{ (GeV}/c)^2$  [reaction (3)] was estimated by fitting the  $p\pi^+$  invariant mass  $M_{p\pi^+}$  to an expression of the form

$$\frac{d\sigma}{dM_{p\pi^+}} = \text{BG} (1 + a \cdot \text{BW}) \quad (4)$$

in the  $1.08 < M_{p\pi^+} < 1.72 \text{ GeV}/c^2$  mass range. In this formula:

$$\text{BW} = \frac{M_{p\pi^+}}{Q(M_{p\pi^+})} \cdot \frac{\Gamma(M_{p\pi^+})}{(M_{p\pi^+}^2 - M_\Delta^2)^2 + (M_\Delta \Gamma(M_{p\pi^+}))^2}$$

\* This  $t$ -cut ensures that the momentum spectrum of the protons arising from  $\Delta^{++}$ -decay does not extend above 1.2 GeV/c

stands for a  $P$ -wave relativistic Breit-Wigner function with

$$\Gamma(M_{p\pi}) = \Gamma_T \left( \frac{Q(M_{p\pi})}{Q(M_{\Delta})} \right)^3 \frac{\varrho(M_{p\pi})}{\varrho(M_{\Delta})}$$

$$\varrho(M) = \frac{(M + m_p)^2 - m_\pi^2}{M^2},$$

$M_{\Delta} = 1.236$  GeV,  $\Gamma_T = 0.12$  GeV and  $Q(M)$  is the momentum of the assumed  $\Delta^{++}$ -decay products in the rest frame of the  $p\pi^+$  system of mass  $M$ . The background (BG) can be satisfactorily represented by an expression of the type already used in a similar analysis performed at a primary momentum of 32 GeV/c [5], namely

$$\text{BG} = \alpha_1 (M - M_{th})^{\alpha_2} \cdot \exp[-\alpha_3 (M - M_{th}) - \alpha_4 (M - M_{th})^2].$$

This exponential background parametrization was chosen as it was found to provide better fits than polynomial representations.

As for  $|t_{p\Delta}| < 0.6$  (GeV/c)<sup>2</sup>, the protons arising from  $\Delta^{++}$ -decay have momenta below 1.2 GeV/c, only those  $p\pi^+$  combinations containing identified protons were considered and were weighted according to the slow proton identification probability. From the results of this fit (see Fig. 2) we estimate

$$\sigma(\Delta^{++}) = (0.68 \pm 0.06) \text{ mb for } |t_{p\Delta}| < 0.6 \text{ (GeV/c)}^2.$$

For the sake of comparison with other experiments, the cross section estimate for  $\Delta^{++}$ -production was extended to the region  $(0.6 \leq t_{p\Delta} < 1)$  (GeV/c)<sup>2</sup> by applying the same fitting procedure as described above but assuming all positive secondaries with momenta above 1.2 GeV/c in turn to be protons and considering all possible  $(p\pi^+)$  mass combinations. The result is  $\sigma(\Delta^{++}) = (0.89 \pm 0.12)$  mb for  $|t_{p\Delta^+}| < 1$  (GeV/c)<sup>2</sup> in agreement with the value expected from the semi-empirical formula:  $\sigma(\Delta^{++}) = (6.1 p_K^{-1} + 0.8)$  mb (with  $p_K$  in units of GeV/c) derived from a fit to similar data obtained at lower and higher (147 GeV/c) beam momenta [6]. A dependence of this type is expected from Reggeon ( $p_K^{-\alpha}$ ) and Pomeron (constant cross section) exchange contributions at the beam vertex. The  $\sigma(\Delta^{++})$  value obtained suggests the dominance of the latter in the present experiment.

The hypothesis of factorization predicts that the ratio of the inclusive  $\Delta^{++}$  cross section to the total cross section be equal for  $pp$  and  $K^+p$  interactions. For  $|t_{p\Delta}| < 1$  (GeV/c)<sup>2</sup> we find

$$\frac{\sigma(K^+p \rightarrow \Delta^{++} + X)}{\sigma_{\text{tot}}(K^+p)} = 0.048 \pm 0.006$$

which compares satisfactorily with the corresponding ratio of  $0.059 \pm 0.006$  determined by a similar experimental method for  $pp$  interactions at 69 GeV/c [7].

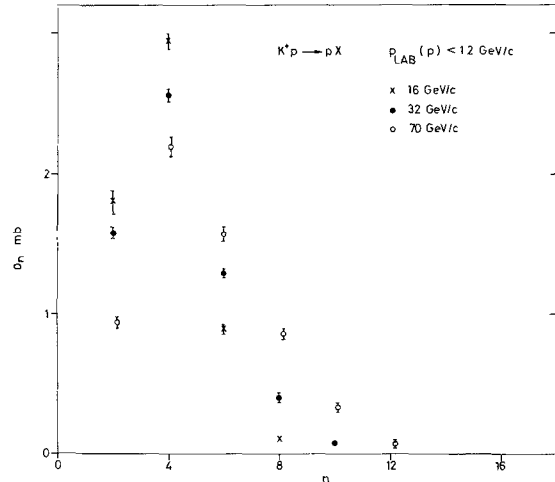


Fig. 1. Topological cross sections for reaction  $K^+p \rightarrow pX$  with  $p_{\text{LAB}}(p) < 1.2$  GeV/c at 16, 32, and 70 GeV/c

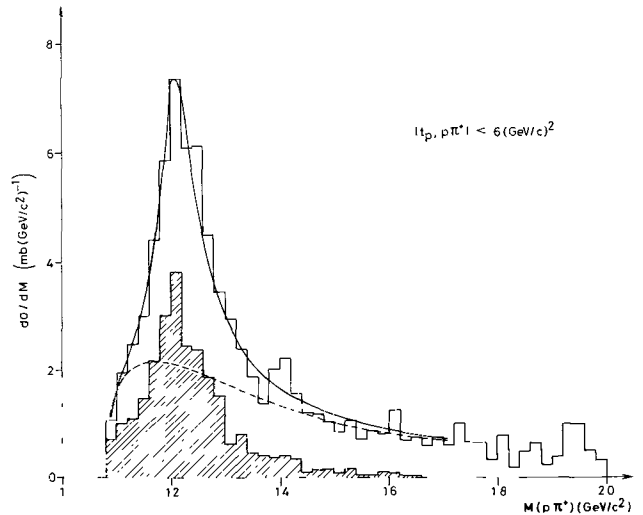


Fig. 2. Inclusive  $(p\pi^+)$  effective mass distribution for events with  $|t_{p, p\pi^+}| < 0.6$  (GeV/c)<sup>2</sup> and an identified proton. The full curve represents the results of the fit to expression (4), the dashed line showing the background contribution. The hatched area corresponds to events with  $\cos\theta_j > 0$

### 3. Differential Cross Sections

The invariant structure function integrated over transverse momentum squared

$$f(x) = \frac{1}{\pi} \int \frac{E^*}{p_{in}^*} \frac{d^2\sigma}{dp_T^2 dx} dp_T^2$$

is shown in Fig. 3 for reactions (1) and (2). In the proton distribution one clearly sees a diffraction peak near  $x \sim -1$ . The  $x$ -distributions in the region  $x \sim -0.8 \div -0.7$  are rather flat for both reactions; in this region the ratio  $f(p)/f(\Delta^{++})$  is about 3. The cross section ratio at higher values is biased due to the cut on the laboratory proton momentum at 1.2 GeV/c.

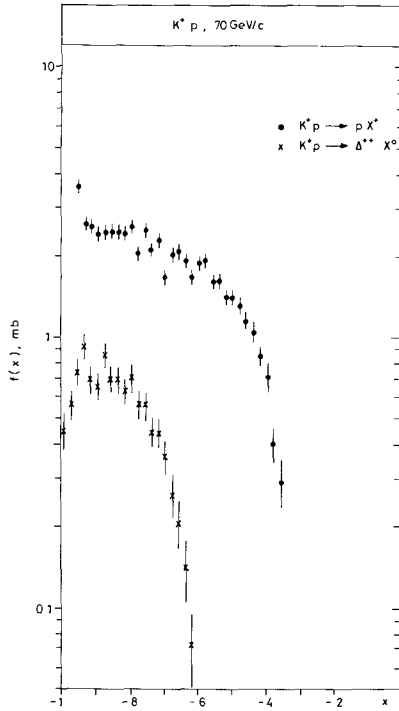


Fig. 3. Invariant structure function  $f(x) = \frac{1}{\pi} \int \frac{E^*}{p_m^*} \frac{d^2\sigma}{dx dp_T^2} dp_T^2$  for reactions (1):  $K^+p \rightarrow pX^+$  and (2):  $K^+p \rightarrow p\pi^+X^+$  at 70 GeV/c

The invariant structure function for reaction (1) averaged over different  $p_T^2$  intervals is shown in Fig. 4. A pronounced diffractive peak is seen up to  $p_T^2 = 0.4 (\text{GeV}/c)^2$ . In this figure we also compare these distributions to similar ones obtained in the inclusive reactions:

$$pp \rightarrow p + X^+ \quad (5)$$

at the incident momentum 69 GeV/c [7] and  $K^+p \rightarrow p + X^+$  at 32 GeV/c [3], renormalizing the total cross sections of both reactions to the total  $K^+p$  cross section at 70 GeV/c. The results are in approximate agreement with the factorization predictions and with scaling.

In Fig. 5 we present the distribution of the missing mass squared  $M_X^2$  with respect to the proton. Figure 6 shows a break-down of this distribution for different charged particle topologies. The diffractive low mass enhancement at  $M_X^2 < 10 (\text{GeV}/c^2)^2$  is clearly seen with dominant contribution from 2- and 4-prong events. Figure 5 shows a quite good agreement between the  $M_X^2$ -distributions for reactions (1) and (5), when the latter is renormalized to the total  $K^+p$  cross section. In Fig. 7 we compare our inclusive data on reaction (1) with the results of a simplified triple Regge para-

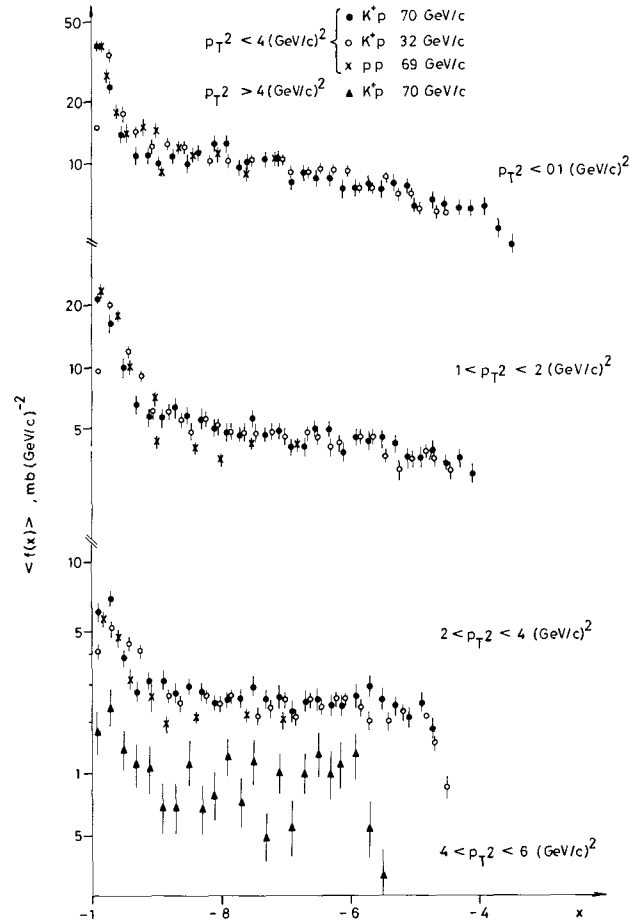


Fig. 4. Average invariant structure function  $\langle f(x) \rangle$  for the reaction  $K^+p \rightarrow pX^+$  at 70 GeV/c vs. The Feynman  $x$ -variable in different  $p_T^2$  intervals. Similar results for the reactions  $K^+p \rightarrow pX^+$  at 32 GeV/c and  $pp \rightarrow pX^+$  at 69 GeV/c, renormalized to the total  $K^+p$  cross section at 70 GeV/c, are also displayed for  $p_T^2 < 0.4 (\text{GeV}/c)^2$

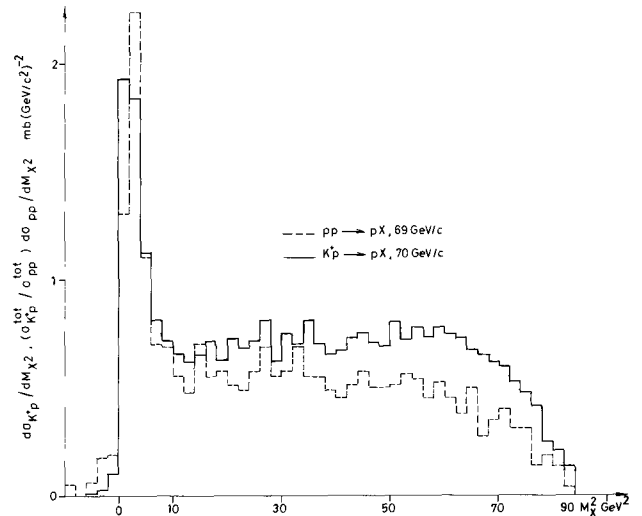
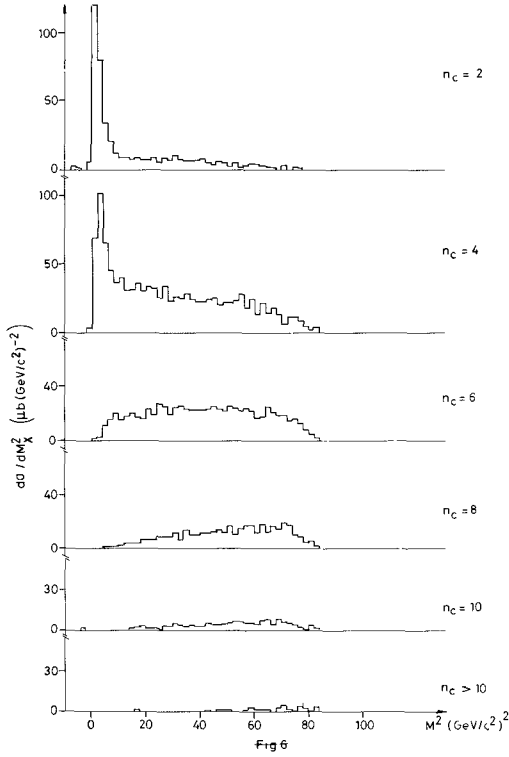


Fig. 5. Comparison of the invariant mass spectra  $M_X^2$  of the system  $X$  in the reactions  $K^+p \rightarrow pX^+$  at 70 GeV/c and  $pp \rightarrow pX^+$  at 69 GeV/c



**Fig. 6.** Invariant mass spectrum of the system  $X$  observed in the reaction  $K^+p \rightarrow pX$  at 70 GeV/c as a function of charged topology  $n_c$ .

metrization of similar data at 16 and 32 GeV/c [3]

$$\frac{d^2\sigma}{dtd(M_X^2/s)} = a(s, t) (M_X^2/s)^{-b(t)} \quad (6)$$

with

$$a(s, t) = G(t) s^{\alpha(0) - 1}. \quad (7)$$

The  $d^2\sigma/dtd(M_X^2/s)$  distributions for different  $t$  intervals are well described by the results obtained in the 32 GeV/c experiment. This indicates that the effective intercept  $\alpha(0)$  is approximately equal to 1 in the region (32–70) GeV/c, and that the “effective” exponent  $b(t)$  is also nearly independent of  $s$ . In order to check whether the latter is true we have fitted expression (6) to our data for  $0.08 < M_X^2/s < 0.4$ , assuming the parameters  $a$  and  $b$  to be constant within each of the  $t$ -intervals shown. The results displayed on Fig. 7 and in Table 2 are in reasonable agreement with the combined results of the 16 and 32 GeV/c data. This again indicates dominance of Pomeron exchange at the beam vertex in reaction (1) between 16 and 70 GeV/c.

The average charged multiplicity  $\langle n_c \rangle$  of the recoiling system  $X$  in the reaction (1) as a function of  $M_X^2$  is presented in Fig. 8. We observe that the de-

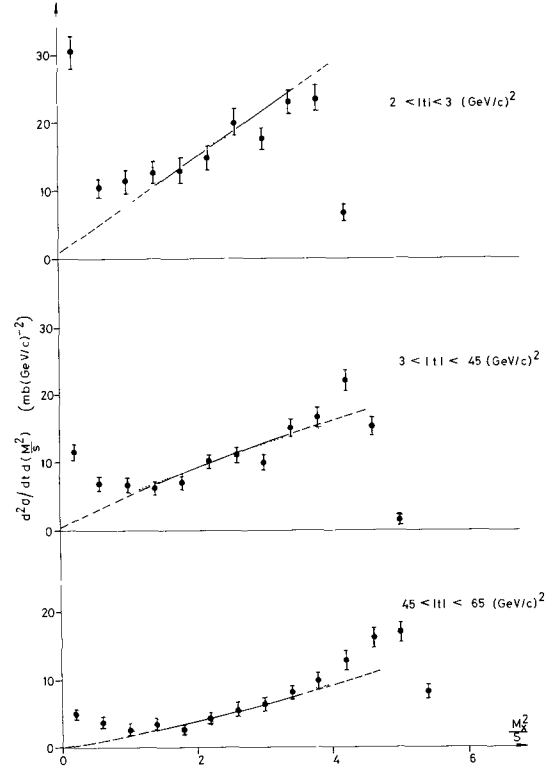


**Fig. 7.**  $d^2\sigma/dtd(M^2/s)$  distributions for different  $t$  intervals in the reaction  $K^+p \rightarrow pX$  at 70 GeV/c. The solid lines represent a simplified triple Regge parametrization made at 32 GeV/c. The dotted line is the same parametrization fitted at 70 GeV/c

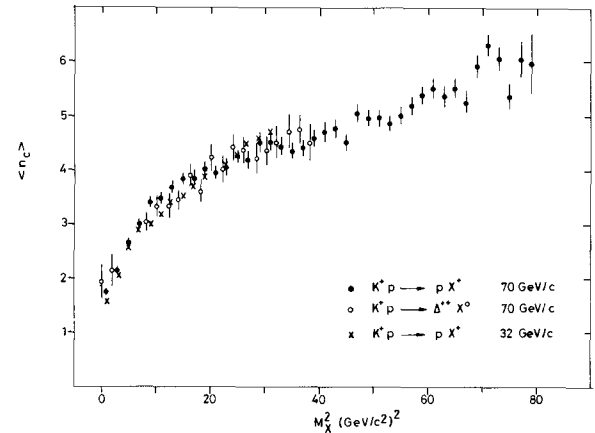


**Fig. 8.** Average charged multiplicity of the recoiling system  $X$  in the reaction  $K^+p \rightarrow pX$  at 32 and 70 GeV/c and  $K^+p \rightarrow \Delta^{++}X$  at 70 GeV/c as a function of its mass squared

**Table 2.** Comparison of the slope values  $b(t)$  of expression (6) (see text) obtained at 70 GeV/c with values obtained at 16 and 32 GeV/c

$ t $ (GeV/c) <sup>2</sup>	$b(t)$ for $p_K=16$ and 32 GeV/c combined	This experiment	
		$b(t)$	$\chi^2/\text{NDF}$
0.2–0.3	$-0.93 \pm 0.07$	$-0.60 \pm 0.09$	6.9/6
0.3–0.45	$-0.96 \pm 0.08$	$-0.83 \pm 0.10$	13.9/6
0.45–0.6	$-1.2 \pm 0.1$	$-1.07 \pm 0.14$	11.3/6

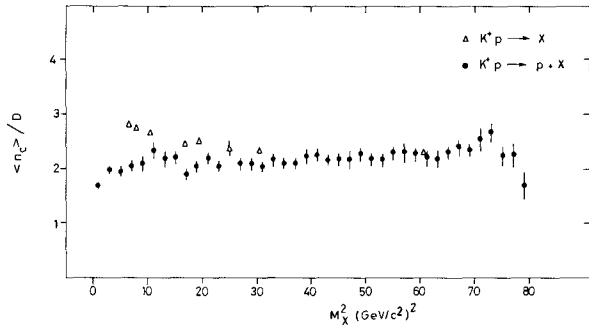


**Fig. 9.** Variation of the  $\langle n_c \rangle / D$  ratio as function of the missing mass squared recoiling against the proton compared to the values obtained for the total multiplicity distributions

pendence of  $\langle n_c \rangle$  on  $M_X^2$  practically coincides with the one observed at 32 GeV/c [3] in the region where both overlap. The average multiplicity of the system recoiling against the " $\Delta^{++}$ " [reaction (2)] follows approximately the same trend, underlining the universal character of these results. Figure 9 displays the  $\langle n_c \rangle / D$  ratio observed for reaction (1) as a function of  $M_X^2$ . No evidence is seen for the existence of a pronounced structure for  $M_X^2 < 10 \text{ GeV}^2$ , as observed in  $\bar{p}p$  interactions at 24 GeV/c [8]. On the contrary, this ratio, as well as the skewness of the distributions (not shown), appear to be constant with values compatible with the universal values of 2.2 and 0.6 respectively as observed in [9]. However, the asymptotic value of

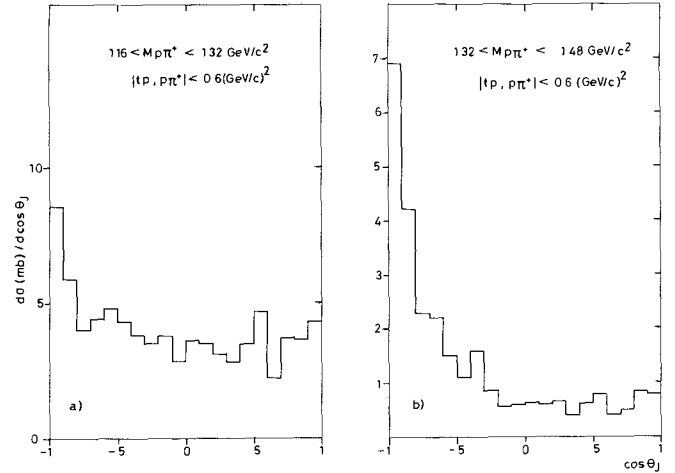


**Fig. 11a and b.** Distributions of the polar Jackson angle in the reaction  $K^+p \rightarrow p\pi^+ + X$  for events with  $|t_{p, p\pi^+}| < 0.6 (\text{GeV}/c)^2$  and a  $(1.16 < M_{p\pi^+} < 1.32) \text{ GeV}/c^2$ , **b**  $(1.32 < M_{p\pi^+} < 1.48) \text{ GeV}/c^2$

$\langle n_c \rangle / D$  is reached from below for reaction (1) (see Fig. 9 and [9]). It is noteworthy that this behaviour is comparable to the one observed for the total charged multiplicity in  $\bar{p}p$  interactions, where a system of baryon number zero is also created.

The four momentum transfer  $d\sigma/dt$ ,  $d\sigma/dt'$  and transverse momentum squared  $d\sigma/dp_T^2$  distributions for reactions (1) and (2) are presented in Fig. 10. They are consistent with exponential parametrizations of the

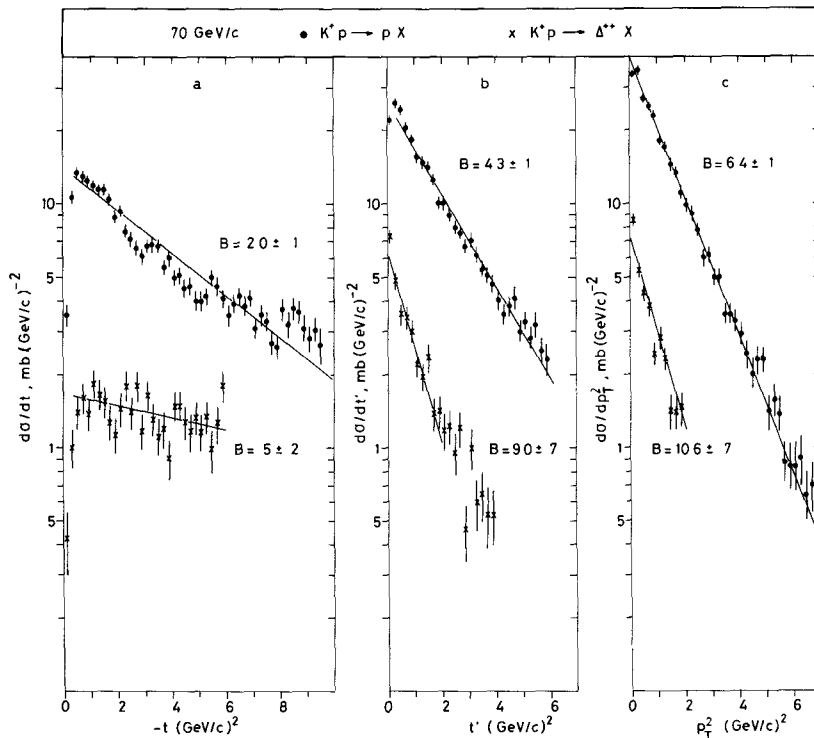


**Fig. 10a-c.** Differential cross sections: **a**  $d\sigma/dt$ ; **b**  $d\sigma/dt'$ ,  $t' = |t - t_{\text{min}}|$ ; **c**  $d\sigma/dp_T^2$  for reactions (1) and (2) at 70 GeV/c

**Table 3.** Results of fits of exponential expressions  $A \exp(-Bz)$  with  $z \equiv -t, t'$  or  $p_T^2$  to the differential cross section data of reactions (1) and (2)

Reaction	Distribution	Fitted interval (GeV/c) <sup>2</sup>	$A$ mb GeV <sup>-2</sup>	$B$ (GeV/c) <sup>-2</sup>
$K^+p \rightarrow p + X^+$ (1)	$d\sigma/dt$	$0.04 \leq -t < 0.96$	$13.3 \pm 0.3$	$2.0 \pm 0.1$
	$d\sigma/dt'$	$0.06 < t' < 0.6$	$25.9 \pm 0.7$	$4.3 \pm 0.1$
	$d\sigma/dp_T^2$	$0.02 < p_T^2 < 0.68$	$39.2 \pm 0.7$	$6.4 \pm 0.1$
$K^+p \rightarrow (p\pi^+) + X^0$ $1.16 \leq M_{p\pi^+} \leq 1.32$ GeV/c <sup>2</sup> (2)	$d\sigma/dt$	$0.06 \leq -t < 0.6$	$1.6 \pm 0.1$	$0.5 \pm 0.2$
	$d\sigma/dt'$	$t' < 0.2$	$6.6 \pm 0.4$	$9.0 \pm 0.7$
	$d\sigma/dp_T^2$	$p_T^2 < 0.2$	$8.0 \pm 0.4$	$10.6 \pm 0.7$

type  $d\sigma/dz = A \exp(-Bz)$  with  $z \equiv t, t'$  or  $p_T^2$ . The results of  $\chi^2$ -fits to these expressions are displayed in Table 3.

The value of the slope  $B = 2.0 \pm 0.1$  (GeV/c<sup>-2</sup>) found for the  $d\sigma/dt$  distribution of reaction (1) is in excellent agreement with the corresponding values determined at 16 GeV/c [ $B = 2.1 \pm 0.03$  (GeV/c)<sup>-2</sup>] and 32 GeV/c [ $B = 2.0 \pm 0.1$  (GeV/c)<sup>-2</sup>] [3].

The  $d\sigma/dt$  distribution for reaction (1) is almost flat. This is obviously due to the  $t_{\min}$  effect for high recoil masses of the  $\Delta^{++}$  and to the fact that the contribution of quasi-two body reactions with low recoil masses is smaller than at lower energies. The steepness of the corresponding  $t'$  distribution suggests that the  $\Delta^{++}$ -production mechanism is peripheral as will be further discussed in the next section.

#### 4. Spin Density Matrix Analysis of $\Delta^{++}$ -Production

The distributions of the polar emission angle  $\theta_J$  of the proton in the Gottfried-Jackson frame of  $(p\pi^+)$ -systems with  $1.16 < M_{p\pi^+} < 1.32$  GeV/c<sup>2</sup> and  $1.32 < M_{p\pi^+} < 1.48$  GeV/c<sup>2</sup> are shown in Fig. 11a and b respectively for  $|t_{p, p\pi^+}| < 0.6$  (GeV/c)<sup>2</sup>. A quite strong forward-backward asymmetry is observed in the  $\Delta^{++}$ -region. However, this asymmetry is much more pronounced when background events are selected in the adjacent control region ( $1.32 < M_{p\pi^+} < 1.48$ ) GeV/c<sup>2</sup>. In the latter case, the  $\cos\theta_J$  distribution is seen to be flat for  $\cos\theta_J > 0$ . Assuming this is also to be the case for background events under the  $\Delta^{++}$ -peak, the data with  $(1.16 < M_{p\pi^+} < 1.32)$  GeV/c<sup>2</sup> and  $|t_{p, p\pi^+}| < 0.6$  (GeV/c)<sup>2</sup> and  $\cos\theta_J > 0$  have been fitted to the decay distribution [10].

$$W_A(\theta_J, \psi_J) = \frac{3}{4\pi} \left\{ \rho_{33} \sin^2\theta_J + \left( \frac{1}{2} - \rho_{33} \right) \left( \frac{1}{3} + \cos^2\theta_J \right) - \frac{2}{\sqrt{3}} \operatorname{Re}\rho_{3-1} \sin^2\theta_J \cos^2\psi_J - \frac{2}{\sqrt{3}} \operatorname{Re}\rho_{31} \sin 2\theta_J \cos\psi_J \right\}.$$

The results are:

$$\rho_{33} = 0.23 \pm 0.08$$

$$\operatorname{Re}\rho_{3-1} = -0.09 \pm 0.08 \quad \text{with} \quad \chi^2/ND = 47/57$$

$$\operatorname{Re}\rho_{31} = 0.05 \pm 0.17.$$

As can be seen from Fig. 2, the  $\Delta^{++}$ -selection after the cut on  $\cos\theta_J > 0$  is particularly clean and it has been checked by imposing an additional  $t'$ -cut that the above results are not sensitive to the remaining background. The values of the spin-density matrix elements found correspond to the ones expected from a triple Regge production model dominated by Pomeron exchange at the kaon vertex and by absorbed pion exchange at the proton vertex [11]. Similar results have been obtained in the 8.2–32.0 GeV/c [4] incident  $K^+$ -momentum range, as well as at 147 GeV/c [6].

#### Conclusions

Our analysis of inclusive and semi-inclusive proton and  $\Delta^{++}$ -production in 70 GeV/c  $K^+p$  interactions leads to the following main results:

1. The inclusive cross section for protons with laboratory momentum less than 1.2 GeV/c is equal to  $(6.1 \pm 0.1)$  mb. The 2-prong and 4-prong cross sections are decreasing in the energy range (16–70) GeV/c while the cross sections at higher charged multiplicities are continuously increasing. The  $x$ -dependence of the proton invariant structure functions in  $K^+p$  reactions at 70 GeV/c and 32 GeV/c and in  $pp \rightarrow pX^+$  at 69 GeV/c is very similar and agrees in absolute value with the hypothesis of scaling and factorization.

A comparison of the 70 GeV/c data for the reaction  $K^+p \rightarrow pX^+$  with a simplified triple-Regge parametrization of this reaction at 16 and 32 GeV/c indicates the dominance of Pomeron exchange at the beam vertex in the (16–70) GeV/c incident momentum range.

2. The inclusive  $\Delta^{++}$ -cross section for  $|t_{p, \Delta}| < 1.0$  GeV/c<sup>2</sup> appears to decrease with the beam momentum, approaching an asymptotic value of  $\sim 0.8$  mb indicative of the dominance of Pomeron over Reggeon

exchanges at the beam vertex at our energy. A comparison of the reactions  $K^+p \rightarrow \Delta^{++}X$  and  $pp \rightarrow \Delta^{++}X$  at the same energy shows evidence for factorization. Absorptive pion exchange at the target vertex is found to provide an adequate interpretation of the spin density matrix elements for  $\Delta^{++}$ -production when described in the framework of a triple Regge model.

*Acknowledgements.* We wish to express our gratitude to the operating crews of the BEBC-chamber and the rf-separating beam. We are also grateful to our scanning, measurement and computing personnel for their diligent work.

## References

1. M. Barth et al.: Z. Phys. C **3**, 285 (1979)
2. I.V. Ajinenko et al.: Nucl. Phys. B **123**, 493 (1977)
3. J. Laurent et al.: Nucl. Phys. B **149**, 189 (1979)
4. P.V. Chliapnikov et al.: Nucl. Phys. B **164**, 189 (1980)
5. J. Granet et al.: Nucl. Phys. B **140**, 389 (1978)
6. D. Brick et al.: Phys. Rev. D **21**, 632 (1980)
7. H. Bialkowska et al.: Nucl. Phys. B **110**, 300 (1976)
8. Alma-Ata – Dubna – Helsinki – Kosica – Moscow – Prague Collaboration: Dubna Preprint EA-12117 (1979)
9. E. De Wolf et al.: Nucl. Phys. B **87**, 325 (1975)
10. K. Gottfried, J.D. Jackson: Nuovo Cimento **33**, 309 (1964)
11. E. Gotsman: Phys. Rev. D **9**, 1575 (1974)